Decentralized Multi-Robot Social Navigation in Constrained Environments via Game-Theoretic Control Barrier Functions

Rohan Chandra[1], Vrushabh Zinage[2], Efstathios Bakolas[2], Joydeep Biswas[1], and Peter Stone[1,*]
{rchandra, vrushabh.zinage, joydeepb, pstone}@utexas.edu, bakolas@austin.utexas.edu
Dept. of Computer Science[1], Dept. of Aerospace Engineering and Engineering Mechanics[2]
The University of Texas at Austin
Full version and videos at **https://amrl.cs.utexas.edu/snupi.html**

***Abstract*— We present an approach to ensure safe and deadlock-free navigation for decentralized multi-robot systems operating in constrained environments, including doorways and intersections. Although many solutions have been proposed to ensure safety, preventing deadlocks in a decentralized fashion with global consensus remains an open problem. In this work, we first formalize the above multi-robot navigation problem in constrained spaces with multiple conflicting agents, which we term as *social mini-games*. To solve social mini-games, we propose a new class of decentralized controllers that ensure both safety and deadlock resolution by attaining a game-theoretic Nash equilibrium. Our controller builds on two key insights: first, we reduce the deadlock resolution problem to solving a modified version of an N-player Chicken game, for which a Nash equilibrium solution exists. Second, we formulate the Nash equilibrium as a control barrier function (CBF) and integrate it with traditional CBFs to inherit their safety guarantees.**

We evaluate our proposed game-theoretic navigation algorithm in simulation as well in the real world using F$1/10$ robots, a Clearpath Jackal, and a Boston Dynamics Spot in a doorway, corridor intersection, roundabout, and hallway scenario. We show that (i) our approach results in safer and more efficient navigation compared to local planners based on geometrical constraints, optimization, multi-agent reinforcement learning, and auctions, (ii) our deadlock resolution strategy is the smoothest in terms of smallest average change in velocity and path deviation, and most efficient in terms of makespan (iii) our approach yields a flow rate of $2.8 - 3.3$ (ms)$^{-1}$ which is comparable to flow rate in human navigation at 4 (ms)$^{-1}$.

I. Introduction

We consider the task of multi-robot navigation in constrained environments such as passing through narrow doors and hallways, or negotiating right of way at corridor intersections. We refer to these types of scenarios as *social mini-games*. Unlike humans, robots often collide or end up in a deadlock due to several challenges arising in social mini-games. Two key challenges, in particular, demand attention. First, without some form of cooperation, decentralized systems, even with perfect local sensing, result in deadlocks, collisions, or non-smooth trajectories. Second, humans are adept at avoiding collisions and deadlocks without having to deviate too much from their preferred walking speed or trajectory, also referred to as *private incentives*. This type of behavior presents a significant challenge for robots, which struggle to emulate such socially adaptive maneuvers while maintaining a consistent preferred velocity. The objective of this paper is to propose a safe, deadlock-free, and incentive compatible navigation algorithm for multiple robots in social mini-games.

The goal is for robots to navigate in such social mini-games as humans do as much as possible. More formally, navigation algorithms must guarantee safety, liveness, and obey kinodynamic constraints. Although multi-robot nabigation encompass a vast range of algorithms, we narrow our focus to algorithms that have been applied to social mini-games either on real robots or in simulation. These include methods based on deep reinforcement learning [1], [2], [3], [4], multi-agent path finding [5], trajectory prediction [6], game-theoretic distributed optimization [7], auctions [8], geometric planning [5], [9], [10], and other optimization-based methods [11], [12], [13], [14], [15]. None of these methods satisfy all of the necessary conditions for optimal multi-robot navigation in social mini-games. In the literature on multi-robot navigation for social mini-games, typically, the problem is that algorithms are either collision-free or deadlock-free, but not both. In a similar vein, algorithms that perform well in simulation, fail when deployed on real robots [16].

Main Contributions: This paper presents a provably safe and deadlock-free multi-robot navigation algorithm for robots with double-integrator dynamics in social mini-games, such as navigating through a narrow door or negotiating right of way at a corridor intersection. Our algorithm is fully decentralized and assumes partial observability. Our main contributions include:

1) A new class of decentralized controllers that ensure both safety and liveness by attaining a game-theoretic Nash equilibrium and can be added to any constrained optimization-based local trajectory planner
2) Our controller builds on two key insights: first, we reduce the deadlock resolution problem to solving a modified version of an N-player "Chicken" game, for which a Nash equilibrium solution exists. Second, we formulate the Nash equilibrium as a control barrier function (CBF) and integrate it with traditional CBFs to inherit their safety guarantees, while simultaneously imbuing it with liveness guarantees.

We show that (i) our approach results in safer and more efficient navigation compared to local planners based on geometrical constraints, optimization, multi-agent reinforcement learning, and auctions, (ii) our deadlock resolution strategy is the smoothest in terms of smallest average change in velocity and path deviation, and most efficient in terms of makespan (iii) our approach yields a flow rate of $2.8 - 3.3$ (ms)$^{-1}$ which is comparable to flow rate in human navigation at 4 (ms)$^{-1}$.

II. Related Work

A. Collision Avoidance

Provable safety can be achieved by single-integrator systems *e.g.* ORCA framework from Van Den Berg et al. [10] and its non-holonomic variant [9], which are effective for fast and exact multi-agent navigation. ORCA conservatively imposes collision avoidance constraints on the motion of a robot as half-planes in the space of velocities. The optimal collision-free velocity can then be quickly found by solving

*Peter Stone is also the Executive Director of Sony AI, America.

a convex optimization problem through linear programming. The original framework limits itself to holonomic systems but has been extended in [9] to model non-holonomic constraints with differential drive dynamics. ORCA also generates collision-free velocities that deviate minimally from the robots' preferred velocities. The major limitation of the ORCA framework is that the structure of the half-planes so constructed often results deadlocks.

Exact safety is harder to prove for higher-order dynamics such as double-integrator dynamics, therefore safety in these systems depend on the planning frequency of the system. For example, the NH-TTC algorithm [15] uses gradient descent to optimize a cost function comprising of a goal reaching term and a time-to-collision term, which rises to infinity as the agent approaches immediate collision. NH-TTC guarantees safety in the limit as the planning frequency approaches infinity. Other optimization-based approaches use model predictive control (MPC) [14] and safety depends not only on the planning frequency but also on the length of the planning horizon.

Finally, control barrier functions (CBFs) [11], [13] guarantee safety via the notion of forward invariance *i.e.* if an agent starts out in a safe set at the initial time step, then it would be safe for all future time steps.

B. Deadlock Resolution Methods

Deadlocks among agents arise due to symmetry in the environment that may cause conflicts between the agents [11], [14], [17]. To break the symmetry, and escape the deadlock, agents must be perturbed, which can be done in several ways. The most naive, and easiest, way is to randomly perturb each agent [13]. Random perturbations can be implemented in decentralized controllers and can generalize to many agents, but are sub-optimal in terms of path deviation and overall cost. Next, there are several recent efforts to choreograph the perturbation according to some set rules such as the right-hand rule [14], [18] or clockwise rotation [11]. These strategies improve optimality over random perturbation and even give formal guarantees, but the imposed pre-determined ordering limits their generalizability; many cannot generalize to more than 3 agents. Another line of research aims towards deadlock *prevention* rather than resolution where an additional objective is to identify and mitigate potential deadlocks, even before they happen, such as in [14].

Another class of deadlock resolution methods rely on priority protocols and scheduling algorithms similar to those used in the autonomous intersection management literature [19]. Some prominent protocols include first come first served (FCFS), auctions, and reservations. FCFS [20] assigns priorities to agents based on their arrival order at the intersection. It is easy to implement but can lead to long wait times and high congestion if multiple vehicles arrive at the intersection simultaneously. In auctions [21], [22], agents bid to cross the intersection based on a specific bidding strategy. Reservation-based systems [23] are similar to the auction-based system in which agents reserve slots to cross the intersection based on their estimated arrival and clearance times.

As noted by recent researchers [14], [18], developing a provably optimal, decentralized, and general deadlock resolution technique is currently an open problem. In this work, we take a large step forward towards a solution.

C. Learning-based Approaches

We refer the reader to [24] for a recent survey on the state-of-the-art of learning-based motion planning. Deep reinforcement learning (DRL) has been used to train navigation policies in simulation for multiple robots in social mini-games. Long et al. [1] presents a DRL approach for multi-robot decentralized collision avoidance, using local sensory information. CADRL [2], or Collision Avoidance with Deep Reinforcement Learning, is a state-of-the-art motion planning algorithm for social robot navigation using a sparse reward signal to reach the goal and penalizes robots for venturing close to other robots. Planning algorithms that use trajectory prediction models [6] estimate the future states of the robot in the presence of dynamic obstacles and plan their actions accordingly.

D. Game-theoretic Distributed Optimization

Another class of methods for multi-agent planning for self-interested agents includes distributed optimization in general-sum differential games. The literature on general-sum differential games classify existing algorithms for solving Nash equilibria in robot navigation into four categories. First, there are algorithms based on decomposition [25], [26], such as Jacobi or Gauss-Siedel methods, that are easy to interpret and scale well with the number of players, but have slow convergence and may require many iterations to find a Nash equilibrium. The second category consists of algorithms based on dynamic programming [27], such as Markovian Stackelberg strategy, that capture the game-theoretic nature of problems but suffer from the curse of dimensionality and are limited to two players. The third category consists of algorithms based on differential dynamic programming [28], [29], [30], [31], [32], [33] that scale polynomially with the number of players and run in real-time, but do not handle constraints well. Lastly, the fourth category contains algorithms based on direct methods in trajectory optimization [7], [34], [35], such as Newton's method, that are capable of handling general state and control input constraints, and demonstrate fast convergence. The algorithms described above give an analytical, closed-form solution that guarantees safety but not liveness, and does not model self-interested agents. Additional limitations include the lack of deployability in the real world and the requirement of full observation.

III. Problem Formulation and Background

In this section, we begin by formulating social mini-games followed by stating the problem objective.

A. Problem Formulation

We formulate a social mini-game by augmenting a partially observable stochastic game (POSG) [36]: $\left\langle k, \mathcal{X}, \{\Omega^i\}, \{\mathcal{O}^i\}, \{\widetilde{\Gamma}^i\}, \mathcal{T}, \{\mathcal{U}^i\}, \{\mathcal{J}^i\} \right\rangle$ where k denotes the number of robots. Hereafter, i will refer to the index of a robot and appear as a superscript whereas t will refer to the current time-step and appear as a subscript. The general state space $\mathcal{X}$ (*e.g.* SE(2), SE(3), etc.) is continuous; the i^{th} robot at time t has a state $x_t^i \in \mathcal{X}$. A state x_t^i consists of both visible parameters (*e.g.* current position and velocity) and hidden parameters which could refer to the internal state of the robot such as preferred speed, preferred heading, etc. We denote the set of observable parameters as $\overline{x}_t^i$. On arriving at a current state x_t^i, each robot generates a local observation, $o_t^i \in \Omega^i$, via $\mathcal{O}^i : \mathcal{X} \longrightarrow \Omega^i$, where $\mathcal{O}^i\left(x_t^i\right) = \left\{x_t^i, \overline{x}_t^j\right\}$ for all $j \in \mathcal{N}\left(x_t^i\right)$, the set of robots detected by i's sensors. Over a finite horizon T, each robot is initialized with a start state $x_0^i \in \mathcal{X}_I$, a goal state $x_T^i \in \mathcal{X}_g$ where $\mathcal{X}_i$ and $\mathcal{X}_g$ denote the sets containing the initial and final states. A discrete trajectory is specified as the vector $\Gamma^i = \left(x_0^i, x_1^i, \ldots, x_T^i\right)$

and its corresponding input sequence is denoted by $\Psi^i = \left(u_0^i, u_1^i, \ldots, u_{T-1}^i\right)$. We denote $\widetilde{\Gamma}^i$ as the set of *preferred* trajectories for robot i that solve the two-point boundary value problem. More formally, due to the local Lipschitz continuity assumption on f and g, for every state $x_t^i \in \widetilde{\Gamma}^i$, there exists $t' \leq T$ such that $x_t^i \in \mathcal{R}\left(x_t^i, \mathcal{U}^i, t'\right) \cap \widetilde{\Gamma}^i$, where $\mathcal{R}\left(x_t^i, \mathcal{U}^i, t'\right)$ is the set of reachable states from x_t^i traveling for time t'. A preferred trajectory refers to a trajectory a robot would follow in the absence of dynamic or static obstacles and is generated via a default planner according to some predefined criteria such as shortest path, minimum jerk, etc. The transition function is given by $\mathcal{T} : \mathcal{X} \times \mathcal{U}^i \longrightarrow \mathcal{X}$, where $u_t^i \in \mathcal{U}^i$ is the continuous control space for robot i. Robots follow the control-affine kinodynamics,

$$\dot{x}^i = f\left(x_t^i\right) + g\left(x_t^i\right) u_t^i \tag{1}$$

where f and g are locally Lipschitz continuous functions. Each robot has a running cost $\mathcal{J}^i : \mathcal{X} \times \mathcal{U}^i \longrightarrow \mathbb{R}$ that assigns a cost to a control u_t^i at each time step based on (i) distance of the robots current position from the goal, (ii) change in the control across subsequent time steps and (iii) difference between the robots preferred and actual paths.

In addition to describing the tuple above, we also define a collision. Represent the space occupied by robot i (as a subset of the state space $\mathcal{X}$) at any time t by its convex hull as $\mathcal{C}^i\left(x_t^i\right) \in \mathcal{X}$. Then, robots i and j are said to collide at time t if $\mathcal{C}^i\left(x_t^i\right) \cap \mathcal{C}^j\left(x_t^j\right) \neq \emptyset$. Finally, we define a social mini-game as follows,

Definition 1. *A **social mini-game** occurs if for some $\delta \in \mathbb{R}^{>0}$ and integers $a, b \in (0, T)$ with $b - a > \delta$, there exists at least one pair $i, j, i \neq j$ such that for all $\Gamma^i \in \widetilde{\Gamma}^i, \Gamma^j \in \widetilde{\Gamma}^j$, we have $\mathcal{C}^i\left(x_t^i\right) \cap \mathcal{C}^j\left(x_t^j\right) \neq \emptyset \; \forall \; t \in [a, b]$, where x_t^i, x_t^j are elements of $\Gamma^i, \Gamma^j \in \widetilde{\Gamma}^i, \widetilde{\Gamma}^j$.*

We depict several examples and non-examples of social mini-games in Figure 1. The first scenario can be characterized as a social mini-game due to the conflicting preferred trajectories of agents 1 and 2 within a specific time interval $[a, b] \in T$, where the duration $b - a \geq \delta$. In this case, the agents' trajectories intersect and result in conflicting paths. However, the second and third scenarios, in contrast, do not qualify as social mini-games since no conflicts arise between the agents. In the second scenario, there is no common time duration where agents intersect each other, and their trajectories remain independent in time. In the third scenario, agent 2 possesses an alternative preferred trajectory that avoids conflicts during any time duration, allowing for a seamless transition to a conflict-free path. A robot has the following best response in a social mini-game,

Definition 2. ***Best Response for a Robot in Social Mini-Games:** For the i^{th} robot, given its initial state x_0^i, an optimal trajectory $\Gamma^{i,*}$ and corresponding optimal input sequence $\Psi^{i,*}$ is given by,*

$$\left(\Gamma^{i,*}, \Psi^{i,*}\right) = \arg\min_{\left(\Gamma^i, \Psi^i\right)} \sum_{t=0}^{T-1} \mathcal{J}^i\left(x_t^i, u_t^i\right) + \mathcal{J}_T^i\left(x_T^i\right) \tag{2a}$$

$$s.t \;\; x_{t+1}^i = f\left(x_t^i\right) + g\left(x_t^i\right) u_t^i, \quad \forall t \in [1; N-1] \tag{2b}$$

$$\mathcal{C}^i\left(x_t^i\right) \cap \mathcal{C}^j\left(x_t^j\right) = \emptyset \; \forall j \in \mathcal{N}\left(x_t^i\right) \tag{2c}$$

$$x_0^i \in \mathcal{X}_i \tag{2d}$$

$$x_T^i \in \mathcal{X}_g \tag{2e}$$

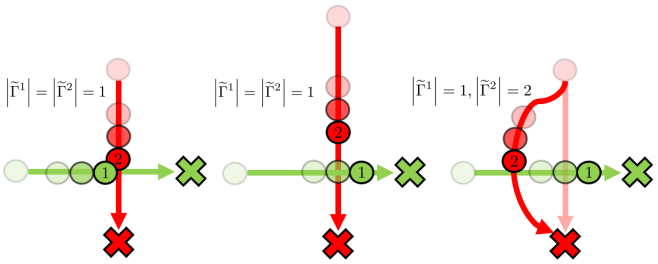

Fig. 1: **Examples/Non-examples of social mini-games:** The first scenario is a social mini-game since both the preferred trajectories of agents 1 and 2 are in conflict from some $t = a$ to $t = b$ where $b - a \geq \delta$. The second and third scenarios are *not* social mini-games as there are no conflicts. In the second scenario, there is no common duration where agents intersect one another. In the third scenario, agent 2 has an alternate conflict-free preferred trajectory to fall back on.

where Equation 2b is a discretized version of Equation 1 and $\mathcal{J}_T^i$ is the terminal cost. At this point, we are ready to state our problem objective.

Problem 1. ***Optimal Navigation in Social Mini-Games:** A solution to optimal navigation in social mini-games is a tuple $\left(\Gamma^{1,*}, \Gamma^{2,*}, \ldots, \Gamma^{k,*}\right)$*

The objective function $\mathcal{J}^i$ captures the cost of a robot deviating from its preferred trajectory between the robot i's current position and the position in the preferred trajectory at time $t \in [0, T]$. An example of such a cost function is $\mathcal{J}^i\left(x_t^i\right) = \left\|x_t^i - \widetilde{x}_t^i\right\|^2$.

In practice, the optimization 2 can be solved optimally (if a solution is reached) via a Dynamic Window Approach (DWA) [37], Model predictive Controller (MPC) [38], Control Barrier Functions (CBF) [39], among others. Let $\mathscr{U}_t^i \subset \mathcal{U}^i$ be the set of controls such that Equation 2c holds and robot i is collision-free. Further, let $\pi^i \in \mathcal{K}$ refer to a chosen controller (MPC, DWA etc.) chosen by agent i, where $\mathcal{K}$ denotes the set of possible controllers.

In social mini-games, $\mathscr{U}_t^i$ often ends up being an empty set resulting in deadlocks [13], [14], [18]. As in previous work [11], [13], [17], we define a deadlock as follows,

Definition 3. ***Deadlock:** A robot i executing the controller given by Equation 2 enters a deadlock if, starting at time t, $u_t^i = 0$ for some fixed time period β, while $x_t^i \notin \mathcal{X}_g$.*

If agent i is assumed to be traveling along $\widetilde{\Gamma}^i$, then system 1 is small-time local controllable giving the following corollary,

Corollary 1. *If at time t, $x_t^i \in \widetilde{\Gamma}^i$ and there is no social mini-game occurring at t, then agent i is not in a deadlock.*

Proof. If there is no social mini-game occurring at time t, then by definition 1, there exist some $\widetilde{\Gamma}^i$ that is not in conflict with any other agent j. Also by definition of a preferred trajectory, for every state $x_t^i \in \widetilde{\Gamma}^i$, $\exists t' \leq T$ such that $x_t^i \in \mathcal{R}\left(x_{t-t'}^i, \mathcal{U}^i, t'\right) \cap \widetilde{\Gamma}^i$, where $\mathcal{R}\left(x_{t-t'}^i, \mathcal{U}^i, t'\right)$ is the set of reachable states from $x_{t-t'}^i$ traveling for time t'. Then $x_T^i \in \mathcal{R}\left(x_{t-t'}^i, \mathcal{U}^i, t'\right) \cap \widetilde{\Gamma}^i$ for some $x_{t-t'}^i, t'$. System 1 is therefore small-time local controllable if agent i follows $\widetilde{\Gamma}^i$, implying that a deadlock does not occur. □

Resolving these deadlocks typically involves perturbing

the robots via a perturbation. Commonly used strategies for λ include randomly perturbing [13], [40] the position of a robot causing it to deviate from its preferred trajectories resulting in a sub-optimal controller.

B. Control Barrier Functions

The safety of a set $\mathscr{C}^i$ is closely related to its forward invariance which is a property that requires the system (1) solutions starting from a given set of initial conditions to remain in a desired safe region $\mathscr{C}^i$ for all $t \geq 0$. The basic idea behind CBFs are as follows. Consider a scalar valued function, $h^i : \mathcal{X} \longrightarrow \mathbb{R}$ over the set of states $x_t^i \in \mathcal{X}$ such that the following holds true:

$$\mathscr{C}^i = \left\{x_t^i \in \mathbb{R}^n | h^i\left(x_t^i\right) \geq 0\right\} \tag{3a}$$

$$h^i\left(x_t^i\right) = 0 \ \forall \ x_t^i \in \partial\mathscr{C}^i \tag{3b}$$

$$h^i\left(x_t^i\right) < 0 \ \forall \ x_t^i \in \mathbb{R}^n \setminus \mathscr{C}^i \tag{3c}$$

where $\mathscr{C}^i$ is the safe set and $\partial\mathscr{C}^i$ denotes the boundary of $\mathscr{C}^i$. The time derivative of $h^i\left(x_t^i\right)$ along the state trajectory of agent i (1) is given as

$$\frac{d\left(h^i\left(x_t^i\right)\right)}{dt} = L_f h^i\left(x_t^i\right) + L_g h^i\left(x_t^i\right) u_t^i \tag{4}$$

where $L_f h^i\left(x_t^i\right)$ and $L_g h^i\left(x_t^i\right)$ denotes the Lie derivatives of $h^i\left(x_t^i\right)$ along f and g respectively. Then $h^i\left(x_t^i\right)$ is a CBF if there exists a class $\mathcal{K}_\infty$[1] function κ such that the following holds true

$$\sup_{u_t^i \in U} \ L_f h^i\left(x_t^i\right) + L_g h^i\left(x_t^i\right) u_t^i + \kappa\left(h^i\left(x_t^i\right)\right) \geq 0 \tag{5}$$

We define the safe or collision-free control space over $x_t^i \in \mathcal{X}$ as the set of controls $u_t^i \in \mathscr{U}^i \subseteq \mathcal{U}^i$ such that the following holds

$$L_f h^i\left(x_t^i\right) + L_g h^i\left(x_t^i\right) u_t^i + \kappa\left(h^i\left(x_t^i\right)\right) \geq 0 \tag{6}$$

The set $\mathscr{U}^i$ that guarantees safety is given by

$$\mathscr{U}^i = \{u_t^i \in \mathcal{U}^i \, | L_f h^i\left(x_t^i\right) + L_g h^i\left(x_t^i\right) u_t^i + \kappa\left(h^i\left(x_t^i\right)\right) \geq 0\} \tag{7}$$

Equation 6 is known as the safety barrier constraint or safety barrier certificate. In summary, the set $\mathscr{C}^i \subseteq \mathcal{X}$ (defined by (3)) is guaranteed to be safe if the control input set $\mathscr{U}^i$ (defined by (7)) is non-empty and $u_t^i \in \mathscr{U}^i$.

IV. Game-theoretic Deadlock Resolution

A state is represented as x_t^i at time t of which $p_t^i, \theta_t^i, v_t^i, \omega_t^i \in \mathbb{R}^2 \times \mathbb{S}^1 \times \mathbb{R}^2 \times \mathbb{R}$ represent the current position, heading, linear and angular rates of the i^{th} robot. We propose a perturbation strategy that can be integrated as a CBF constraint and combined with existing controllers, such as MPC or DWA, to resolve deadlocks. Our perturbation strategy is designed to ensure that:

1) the robot does not deviate from the preferred trajectory.
2) the robot performs the perturbation in a decentralized fashion.
3) the robot deviates minimally from its current velocity.

We design a perturbation that acts on v_t^i, and not on p_t^i, through the notion of *liveness sets*, which are analogous to the safety sets in CBFs. More formally,

[1]A function $\alpha(\cdot) : \mathbb{R} \to \mathbb{R}$ belongs to the class of $\mathcal{K}_\infty$ functions if it is strictly increasing and in addition, $\alpha(0) = 0$ and $\lim_{r\to\infty} \alpha(r) = \infty$

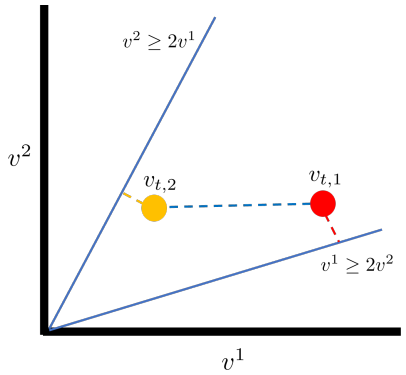

Fig. 2: **Liveness set**($\mathscr{C}_\ell(t)$): for the 2 robot scenario for social mini-games at doorways.

Definition 4. *At any time t, given a configuration of k robots, $x_t^i \in \mathcal{X}$ for $i \in [1, k]$, there exists a union of convex sets, $\mathscr{C}_\ell(t) \in \mathbb{R}^k$ of joint velocity $v_t = \left[v_t^1, v_t^2, \ldots, v_t^k\right]^\top$ such that if $v_t \in \mathscr{C}_\ell(t)$, then a social mini-game does not occur at time t. We call $\mathscr{C}_\ell(t)$ a **liveness set**.*

If every agent at $t = 0$ is collision-free, then perturb u_t^i for all i such that $\mathcal{R}\left(x_t^i, \mathcal{U}^i, \Delta t\right) \cap \widetilde{\Gamma}^i \neq \mathcal{R}\left(\widehat{x}_t^i, \mathcal{U}^i, \Delta t\right) \cap \widetilde{\Gamma}^i$ and $\mathcal{C}^i\left(\widehat{x}_t^i\right) \cap \mathcal{C}^j\left(\widehat{x}_t^j\right) \neq \emptyset \ \forall \ t \in [t, t + \Delta t]$, where $\widehat{x}_{t+\Delta t}^i \in \mathcal{R}\left(\widehat{x}_t^i, \mathcal{U}^i, \Delta t\right) \cap \widetilde{\Gamma}^i$. Trivially, one possible choice is $u_t^j = 0$ for all $j \neq i$ so that $\mathcal{R}\left(\widehat{x}_t^j, \mathcal{U}^j, \Delta t\right) \cap \widetilde{\Gamma}^j = \left\{x_t^j\right\}$ and $\mathcal{C}^i\left(x_t^i\right) \cap \mathcal{C}^j\left(\widehat{x}_t^j\right) \neq \emptyset \ \forall \ t \in [t, t + \Delta t]$ where $\Delta t < \beta$. Consider the resulting set of velocities as $\mathcal{Y} = \left(v_t^1, v_t^2, \ldots, v_t^k\right)$ that precludes a social mini-game. $\mathcal{Y}$ can be convexified by taking the convex hull $conv\left(\mathcal{Y}\right)$. Now, we permute the order of agents $k!$, each resulting in a different convex hull. We take the union of these convex hulls.

Definition 4 and Corollary 1 imply that if each v_t^i is such that the joint velocity $v_t \in \mathscr{C}_\ell(t)$, then there is no deadlock. If, however, $v_t \notin \mathscr{C}_\ell(t)$, then robot i will adjust v_t^i such that v_t is projected on to the nearest point in $\mathscr{C}_\ell(t)$ via,

$$\widetilde{v}_t = \arg \min_{\mu \in \mathscr{C}_\ell(t)} \|v_t - \mu\|_2 \tag{8}$$

Observe that a solution to 8 achieves the first and third objective, that is, agents do not deviate from their preferred path and the new joint velocity $\widetilde{v}_t$ is such that agents deviate minimally from their current joint velocity v_t. Towards the second objective, we show that each agent selects a perturbation strategy that constitutes a Nash solution to a variant of the well-known Chicken game.

Example 1 *(two agents):* While our approach generalizes to k robots, we consider an example with 2 robots for simplicity. In the 2 robot scenario where each robot is equidistant from a doorway or intersection, the liveness set $\mathscr{C}_t^\ell$, shown in Figure 2, is generated by scaling v_t^2 by $\frac{v_t^1}{\zeta}$, or vice-versa. Empirically, it is observed that $\zeta \geq 2$. We can then generate the following system of linear inequalities,

$$v_t^1 \geq \zeta v_t^2$$
$$v_t^2 \geq \zeta v_t^1$$

This can be compactly represented as

$$A_{2\times 2} v_t \geq 0 \tag{9}$$

where $A_{2\times2} = \begin{bmatrix} 1 & -\zeta \\ -\zeta & 1 \end{bmatrix}$ and $v_t = \left[v_t^1, v_t^2\right]^\top$. Suppose the current value of v_t is p_1 as shown in Figure 2. The point $v_{t,1}$ indicates that $A_{2\times2}v_{t,1} < 0$ which lies outside $\mathscr{C}_\ell(t)$, implying that the two robots are in a deadlock according to Definition 4 and Definition 3. Equation 8 projects $v_{t,1}$ onto the nearest half-plane which is the $v_t^1 = \zeta v^2$ barrier. Thus, robot 1 will increase v^1 and robot 2 will decrease v^2 by projecting $v_{t,1}$ down on $v_t^1 = \zeta v^2$. This projection is the minimal deviation required on the part of both robots and is therefore optimal.

Equation 9 can be used to generate the liveness set $\mathscr{C}_\ell(t)$ as,

$$\begin{aligned} \mathscr{C}_\ell(t) &= \{v_t \text{ s.t. } h_v\left(x_t\right) \geq 0\} \\ h_v(x_t) &= \bar{A}_{k\times k}\left(x_t\right) \end{aligned} \tag{10}$$

where $h_v\left(x_t\right)$ is the CBF of $\mathscr{C}_\ell(t)$ that ensures the forward invariance of $\mathscr{C}_\ell(t)$, $x_t = \left[p_t^1, v_t^1, \theta_t^1, \omega_t^1, p_t^2, v_t^2, \theta_t^2, \omega_t^2\right]^\top$ and controls, $u_t = \left[u_t^1, u_t^2\right]^\top$. Following the 2 agent example, we can expand the matrix $A_{2\times2}$ as $\bar{A}_{2\times8} = \begin{bmatrix} 0 & 1 & 0 & 0 & 0 & -\zeta & 0 & 0 \\ 0 & -\zeta & 0 & 0 & 0 & 1 & 0 & 0 \end{bmatrix}$ to accommodate the aggregate of both the robots' states and controls. Combining Equation 10 with Equation 6 using general control-affine dynamics in Equation 1, we can derive the game-theoretic safety barrier constraint. As $h_v\left(x_t\right)$ is a vector field (as opposed to a scalar-valued function),

$$L_f h_v\left(x_t\right) + u_t L_g h_v\left(x_t\right) + \kappa\left(h_v\left(x_t\right)\right) \geq 0 \tag{11}$$

where the Lie derivatives of $h_v(x_t)$ along f and g and inequality above are performed element wise. The best response, $\left(\Gamma^{i,*}, \Psi^{i,*}\right)$, in Equation 2 can be solved by adding Equation 10 in constraint 12c as follows,

$$\arg\min_{(\Gamma^i,\Psi^i)} \sum_{t=0}^{T-1} \left(x_t^i - \widetilde{x}_t^i\right)^{\mathrm{T}} Q\left(x_t^i - \widetilde{x}_t^i\right) + \left(u_t^i\right)^\top R u_t^i + \mathcal{J}_T^i\left(x_T^i\right) \tag{12a}$$

$$\text{s.t} \quad x_{t+1}^i = f\left(x_t^i\right) + g\left(x_t^i\right) u_t^i, \quad \forall t \in [1; N-1] \tag{12b}$$

$$B\left(x_t^i\right) u_t^i \geq C\left(x_t^i\right) \tag{12c}$$

$$\mathcal{C}^i\left(x_t^i\right) \cap \mathcal{C}^j\left(x_t^j\right) = \emptyset \ \forall j \in \mathcal{N}\left(x_t^i\right) \tag{12d}$$

$$x_0^i \in \mathcal{X}_i \tag{12e}$$

$$x_T^i \in \mathcal{X}_g \tag{12f}$$

where $Q \succ 0$ and $R \succ 0$ are positive definite matrices and constraints (12b)-(12d) must be enforced at all times. $B\left(x_t^i\right)$ and $C\left(x_t^i\right)$ are given by

$$B\left(x_t^i\right) = \frac{\partial h\left(x_t^i\right)}{\partial x_i^t} g\left(x_t^i\right), \tag{13a}$$

$$C\left(x_t^i\right) = -\frac{\partial h\left(x_t^i\right)}{\partial x_i^t} f\left(x_t^i\right) - \kappa h\left(x_t^i\right), \tag{13b}$$

$$h\left(x_t^i\right) = \left[h_s(x_t^{i,1}), \ldots, h_s(x_t^{i,N-1}),\ h_v\left(x_t^i\right)\right]^\top, \tag{13c}$$

$$h_s\left(x_t^{i,j}\right) = \left\|p_t^i - p_t^j\right\|_2^2 - r^2, \forall \quad j \in [1; N] \setminus i \tag{13d}$$

$$h_v\left(x_t\right) = \bar{A}_{k\times k}\left(x_t\right) \tag{13e}$$

where $h_s(x_t^{i,j})$ represents the CBF for the agent i which ensures that agent i does not collide with agent j by maintaining a safety margin distance of at least r. In addition, $h_v(x_t^i)$ avoids the problem of deadlocking as $v_t \in \mathscr{C}_\ell(t)$ implies non-existence of a social mini-game. The inverse, however, may not hold true. That is, $v_t \notin \mathscr{C}_\ell(t)$ may not necessarily result in a social mini-game. For example, two agents equidistant from a doorway with equal speeds may prefer to travel parallel to each other. Therefore, perturbing agents' speeds via Equation 8 only if $v_t \notin \mathscr{C}_\ell(t)$ may be an overly conservative approach. We thus introduce the liveliness function $\ell_j\left(p_t^i, v_t^i\right)$ for agent i with respect to the agent j as follows:

$$\ell_j(p_t^i, v_t^i) = \cos^{-1}\left(\frac{\left\langle p_t^i - x_t^j, v_t^i - v_t^j\right\rangle}{\left\|p_t^i - x_t^j\right\| \left\|v_t^i - v_t^j\right\| + \epsilon}\right) \tag{14}$$

where $\left\langle v_t^i, v_t^i\right\rangle$ denotes the dot product between vectors v_t^i and v_t^j and $\epsilon > 0$ is to ensure that the denominator is non-negative. Note that $\ell_j\left(p_t^i, v_t^i\right) \in [0, \pi]$ and $\ell_j\left(x_t^i, v_t^i\right) < \ell_{\text{thresh}}$ implies that i and j are on a collision course. We claim that $\ell_j\left(x_t^i, v_t^i\right) < \ell_{\text{thresh}}$ is a sufficient condition to establish the existence of a social mini-game since according to Definition 1, a social mini-game implies that at $t = a$, there is a collision marking the beginning of the social mini-game. That is, $\exists x_t^i, x_t^j$ for $t < a$ such that $\ell_j\left(x_t^i, v_t^i\right) < \ell_{\text{thresh}}$.

In contrast to traditional CBFs where the CBF $h(x_t^i)$ is usually a function of spatial coordinates such as position only, our proposed CBF $h(x_t^i)$ in (13c) is a function of both position $h_s(x_t^{i,j})$ (defined in (13d)) and velocity $h_v(x_t)$ (defined in (13e)). Unifying these constraints in the formulation of CBF enables robots to simultaneously prevent collisions and deadlocks. Furthermore, for cases of single integrator dynamics where v_t^i is a input, the constraint Av_t (where $v_t = [v_t^1,\ v_t^2]^{\mathrm{T}}$ for two agents) can directly be incorporated in the optimization problem. However in cases of double or higher integrator robotic systems (such as bipedal robots [41], Boston Dynamics Spot etc.), since v_t^i is also a state, guaranteeing the invariance of the set $A_{k\times k}v_t \geq 0$ becomes non trivial.

Theorem 1. *Equation 8 is a mixed-strategy Nash Equilibrium solution.*

Proof. It is known that the classical Chicken game has a mixed-Nash solution when both agents "swerve". We consider the deadlock resolution strategy as solving a version of the Chicken game-if neither agent perturbs their state, then a social mini-game will occur, resulting in a deadlock. The only other alternatives are for either or both of the agents to perturb their current state. As the optimal perturbation solution to Equation 8 requires *both* the agents to perturb their velocities, it corresponds to the mixed-Nash solution of the Chicken game. □

Remark: For $v_t^i \neq v_t^j$ for all i, j, there is always a unique mixed-Nash solution. Consider in example 1 that robot 1 decides to deviate from its current speed in $v_{t,1}$ and decides to decrease its speed, shown by the new point $v_{t,2}$. In that case, robot 2's optimal strategy will no longer be to decrease its speed as before. Now, the nearest safety barrier becomes $v_t^2 = \zeta v^1$, and to project $v_{t,2}$ to this barrier, robot 2 will instead increase its speed. Therefore, assuming a robot does not deviate from its current speed, there will be a unique projection to one of the safety barriers. If $v_t^i = v_t^j$ for some i, j, then there are multiple mixed-Nash solutions and we implement the following tie breaking protocol [42].

V. Evaluation and Discussion

In this section, we deploy our approach in both simulated as well as real world social mini-games occurring at doorways, hallways, intersections, and roundabouts, and investigate the following questions–(i) is the proposed navigation algorithm better at avoiding deadlocks and collisions than the state-of-the-art? (ii) how does the proposed navigation system compare to different approaches such as multi agent reinforcement learning? (iii) is our controller robust to the choice of different kinodynamic local planners? and finally, (iv) how does our game-theoretic deadlock resolution strategy compare to alternative perturbation strategies?

A. Experiment Setup

We numerically validate our approach on differential drive robots in social mini-games that occur at doorways, hallways, intersections, and roundabouts, and analyze its properties. We use the IPOPT solver [43] for solving the MPC optimization. We consider the following differential drive robot:

$$\begin{bmatrix} \dot{p}^{i,1} \\ \dot{p}^{i,2} \\ \dot{\phi}^i \\ \dot{v}^i \\ \dot{\omega}^i \end{bmatrix} = \begin{bmatrix} \cos\left(\phi^i\right) & 0 & 0 & 0 \\ \sin\left(\phi^i\right) & 0 & 0 & 0 \\ 0 & 1 & 0 & 0 \\ 0 & 0 & 1/m & 0 \\ 0 & 0 & 0 & I^{-1} \end{bmatrix} \begin{bmatrix} v^i \\ \omega^i \\ u_1 \\ u_2 \end{bmatrix}, \quad (15)$$

where subscript i denotes the i^{th} agent, m and I are the mass and inertia respectively, $p^{i,1} \in \mathbb{R}$ and $p^{i,2} \in \mathbb{R}$ represent the horizontal and vertical positions of the robot, $\phi^i \in \mathbb{S}^1$ represents its orientation, $[v^i,\ \omega^i] \in \mathcal{U}^i$ are the linear and angular velocity of the robot respectively and $u^i = [u_1,\ u_2]^{\mathrm{T}}$ is the control input. Let the discrete dynamics of (15) be given by

$$x^i_{t+1} = f\left(x^i_t\right) + g\left(x^i_t\right) u^i_t \quad (16)$$

where the sampling time period $T = 0.1s$, $x^i_t = [p^{i,1},\ p^{i,2},\ \phi^i,\ v^i,\ \omega^i]^{\mathrm{T}}$ is the state and $u^i_t = [u_1,\ u_2]^{\mathrm{T}}$ is the control input. The objective is to compute control inputs that minimize the following cost function,

$$\begin{aligned} \min_{u_{1:T-1}} \quad & \sum_{t=0}^{T-1} {x^i_t}^{\top} Q x^i_t + {u^i_t}^{\top} R u^i_t \\ \text{s.t} \quad & x^i_{t+1} = f\left(x^i_t\right) + g\left(x^i_t\right) u^i_t, \quad \forall\, t \in 1, \ldots, T-1 \\ & x_t \in \mathcal{X},\ u_t \in \mathcal{U}^i \quad \forall\, t \in \{1, \ldots, T\} \end{aligned} \quad (17)$$

The safety for the differential drive robot is guaranteed by the CBF constraint (10) For each agent, the CBF for the obstacles is characterized by $h_s\left(x^{i,m}_t\right)$ given by

$$h_s\left(x^{i,m}_t\right) = \left(p^{i,1} - c^{1,m}\right)^2 + \left(p^{i,1} - c^{2,m}\right)^2 - r^2 \quad (18)$$

where $r > 0$, x^i_t is specified by $p^i_t, \theta^i_t, v^i_t, \omega^i_t \in \mathbb{R}^2 \times \mathbb{S}^1 \times \mathbb{R}^2 \times \mathbb{R}$ representing the current position, heading, linear and angular rates of the i^{th} robot and $(c_{1,m}, c_{2,m})$ is the center for circle of radius $r > 0$ and $m \in \{1, \ldots, M\}$ where M is sufficiently large to cover all the obstacles. Therefore, the points lying in the safe region are characterized by the set $\mathcal{X}$ given by

$$\mathcal{X} = \left\{ x^i_t :\ h_s\left(x^{i,m}_t\right) > 0,\ \forall\, m \in \{1, \ldots, M\} \right\} \quad (19)$$

Further to avoid collisions with another agent, each agent i treats the other agent j $(i \neq j)$ as an obstacle. Consequently, the CBF for agent i is given by Equation 13d. The game theoretic CBF $h_v\left(x_t\right)$ for an agent i is given by

$$h_v(x^i_t) = A v_t, \quad i \neq j \quad (20)$$

where $v_t = [v^i_t,\ v^j_t]^{\top}$, $A \in \mathbb{R}^{2\times 2}$. For our doorway and intersection simulations, we choose $A = \begin{bmatrix} -1 & -2 \\ -2 & -1 \end{bmatrix}$.

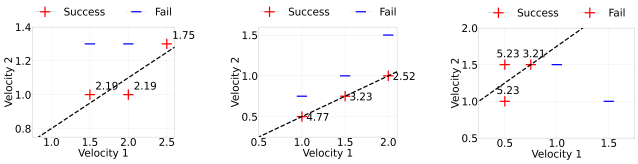

(a) F1/10, door. (b) F1/10, intersection. (c) Spot/Jackal, door.

Fig. 3: **Liveness sets** for 2 F1/10 car platforms, the Clearpath Jackal robot, and the Boston Dynamics Spot robot, in the doorway scenario.

B. Environments and Hardware

Real World– In a 3x3 meter space, experiments were carried out involving two social mini-games at a doorway and intersection. The tests employed three distinct robots: UT Automata F1/10 car platforms, Clearpath Jackal, and Boston Dynamics Spot. Each robot was chosen based on its unique shape, size, and kinodynamic properties. The Spot functions with legs, whereas the Jackal and F1/10 platforms are wheeled, with the Jackal capable of point turns. They have speed capacities of 1.5 m/s and 9 m/s respectively. Notably, the larger robots couldn't detect the cars due to their lower height. The navigation algorithm was benchmarked against a classical DWA planner.
Simulation–We compared our methodology with NH-TTC [15] and NH-ORCA [9] using the SocialGym 2.0 simulator [44], available on Github[2]. We also tested multi-agent reinforcement learning baselines such as CADRL, CADRL(L), and Enforced Order. The CADRL [2] framework and its LSTM variant, CADRL(L), provide rewards for reaching goals while penalizing for collisions or excessive proximity to other robots. Enforced Order is designed to promote social behaviors like queuing. Evaluation metrics used include success rate, time still, and average Δ velocity.

C. Liveness Sets

We generated the liveness sets empirically for both 2-agent and 3-agent social mini-games at doorways and intersections. This involves deploying robot combinations at different speeds in these mini-games, and the range of velocities resulting in safe navigation forms the empirical liveness set for each mini-game. **Doorway with 2 F1/10 Cars**. From Figure 3a, during 5 trial runs averaged over 3 iterations, 3 were successful and 2 failed. Success correlated with velocities adhering to Equation 9. When velocities didn't align with this equation, failures occurred. **Intersection Scenario**. **Cross Robot Platforms**. Validating Equation 9's applicability beyond specific robot models, Figure 3c shows experiments involving the Spot and the Jackal robots in the doorway scenario. This mirrored setups using F1/10 platforms.

D. Real World Experiments

Multi-robot setting–Doorway Scenario. A gap size of about 0.5 meters was set. Robots started from one end

[2]https://github.com/ut-amrl/social_gym

(a) Game-theoretic MPC-CBF (b) MPC-CBF [45] (c) NH-ORCA [9] (d) NH-TTC [15]

Fig. 4: **Liveness in various navigation systems.**

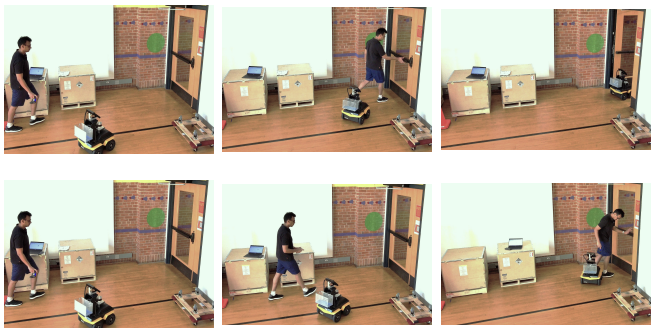

Fig. 5: **Deployment in human-robot environments.**

of the doorway and aimed to move to the opposite side. Their starting positions were either equidistant from the gap (about 1.8 meters apart) or staggered. **Corridor Intersection Scenario**. The width for the four arms of the intersection was set between 1.5 and 2 meters, with a central conflict zone of 2.5 to 4 square meters. A standard autonomous navigation test was executed with one robot per intersection arm. A robot could choose any of the other three arms as its destination.

Our navigation system performed comparably to human navigation. Humans typically move at 1.4 m/s at busy intersections, as per studies [46], [47]. The robots in our tests moved at about 1.25 - 1.5 m/s, exhibiting a flow rate of 2.8 - 3.3 $(\text{ms})^{-1}$.

Human-robot setting–We mirrored the multi-robot doorway test, but with human-robot interaction. Our navigation algorithm was evaluated against a classical DWA planner. In the multi-robot context, outcomes are detailed in Figure 3. DWA planner outcomes aren't shown since robots consistently failed due to collisions or deadlocks. Success or failure of each trial is reported in Figure 3 with the associated makespan times.

E. Simulation Results

Utilizing the game-theoretic MPC-CBF controller, we showcased its application in doorway and intersection scenarios, highlighting a yielding behavior from the green agent to the red one. When compared to the traditional MPC-CBF, our method deftly avoids deadlocks arising from environmental symmetries by making minimal velocity adjustments that align with the Nash equilibrium strategy. This change is triggered by a liveness function when a potential deadlock situation is anticipated. Notably, standard motion planners often result in deadlocks in symmetrical environments. Our algorithm, when compared with DWA and multi-agent reinforcement learning baselines, notably outperforms them. The DWA performed poorly, corroborated by our real-world tests. Our technique also ensures minimal velocity variations, exemplifying smooth navigation. Interestingly, the deadlock solution can be integrated with various controllers without affecting performance.

	Baseline	Success Rate	Coll. Rate	Stop Time	Avg. ΔV
DOOR	CADRL [2]	32 ± 3.125	0.00 ± 0.000	222 ± 2.749	13 ± 1.905
	CADRL(L) [3]	0 ± 0.000	0.12 ± 0.000	436 ± 0.318	36 ± 3.042
	Enforced Ordering	44 ± 2.993	0.16 ± 0.243	617 ± 1.803	117 ± 0.686
	DWA	4 ± 0.244	2.32 ± 0.589	166 ± 4.496	30 ± 2.506
	Auction-based	76 ± 2.270	0.17 ± 0.012	110 ± 4.100	6 ± 1.111
	Game-theoretic QP-CBF	**100±0.000**	**0.00±0.000**	**25±4.235**	**2±0.000**
	Game-theoretic MPC-CBF	**100±0.000**	**0.00±0.000**	**18±1.067**	**2±0.098**
INTER.	CADRL [2]	20 ± 0.453	1.20 ± 0.634	389 ± 5.153	28 ± 1.141
	CADRL(L) [3]	28 ± 2.527	0.32 ± 1.393	267 ± 6.453	127 ± 2.357
	Enforced Ordering	56 ± 0.718	0.80 ± 0.894	233 ± 1.729	104 ± 5.041
	DWA	16 ± 1.765	2.48 ± 0.57	640 ± 4.583	97 ± 2.495
	Auction-based	96 ± 3.342	0.14 ± 0.003	139 ± 5.233	6 ± 0.470
	Game-theoretic QP-CBF	**100± 0.000**	**0.00± 0.000**	**46± 2.349**	**2± 0.040**
	Game-theoretic MPC-CBF	**100± 0.000**	**0.00± 0.000**	**27± 0.140**	**0± 0.000**

TABLE I: **Comparing Game-theoretic MPC-CBF versus baselines.**

	Baseline	Avg. ΔV	Path Deviation	Makespan Ratio
DOORWAY	Random QP-CBF [13]	0.38 ± 0.12	1.874 ± 0.28	2.68 ± 1.00
	ORCA-MAPF [5]	0.10 ± 0.00	0.00 ± 0.00	3.04 ± 0.00
	Game-theoretic QP-CBF [13]	0.22 ± 0.01	0.145 ± 0.00	3.37 ± 0.01
	IMPC-DR [14]	0.08 ± 0.00	0.160 ± 0.00	1.53 ± 0.00
	Game-theoretic MPC-CBF	$\mathbf{0.001 \pm 0.00}$	$\mathbf{0.089 \pm 0.02}$	$\mathbf{1.10 \pm 0.00}$
INTERSECTION	Random QP-CBF [13]	0.30 ± 0.10	0.400 ± 0.14	0.99 ± 0.04
	ORCA-MAPF [5]	0.25 ± 0.00	0.00 ± 0.00	2.22 ± 0.00
	Game-theoretic QP-CBF [13]	0.29 ± 0.05	0.111 ± 0.04	2.24 ± 0.04
	IMPC-DR [14]	0.08 ± 0.00	0.151 ± 0.0	1.13 ± 0.00
	Game-theoretic MPC-CBF	$\mathbf{0.002 \pm 0.00}$	$\mathbf{0.066 \pm 0.01}$	$\mathbf{1.05 \pm 0.01}$
HALLWAY	Random QP-CBF [13]	0.055 ± 0.01	0.327 ± 0.32	1.16 ± 0.04
	ORCA-MAPF [5]	0.11 ± 0.00	1.99 ± 0.00	1.03 ± 0.00
	Game-theoretic QP-CBF [13]	0.008 ± 0.00	0.190 ± 0.00	1.44 ± 0.04
	IMPC-DR [14]	0.135 ± 0.00	0.194 ± 0.00	2.08 ± 0.00
	Game-theoretic MPC-CBF	$\mathbf{0.001 \pm 0.00}$	$\mathbf{0.047 \pm 0.00}$	$\mathbf{1.04 \pm 0.00}$

TABLE II: **Comparing alternate perturbation strategies.**

F. Comparing with Alternate Perturbation Strategies

We tested our game-theoretic deadlock resolution method, Game-theoretic MPC-CBF, against several methods, including a random perturbation technique, a modified version incorporating our game-theoretic approach, an MPC and buffered voronoi cells method, and an ORCA-based method using MAPF for deadlock resolution. The evaluation was done in social scenarios like doorways, hallways, and intersections. Key metrics were the average change in velocity, path deviation, and average time steps across agents. Our game-theoretic approach outperformed in terms of velocity modulation efficiency and trajectory alignment with the preferred path. However, the performance in average completion time varied depending on the specific scenario, with random perturbation occasionally being faster but less efficient in its trajectories.

VI. Conclusion, Limitations, and Future Work

In this work, we presented an approach to address the challenges of safe and deadlock-free navigation in decentralized multi-robot systems operating in constrained environments. We introduced the notion of *social mini-games* to formalize the multi-robot navigation problem in constrained spaces. We proposed a novel class of decentralized controllers capable of guaranteeing both safety and deadlock resolution by achieving a game-theoretic Nash equilibrium.

The main limitation of this work is that the approach assumes the liveness sets are known apriori. Liveness sets can, however, be estimated either in simulation or using learning-based methods for generating cost maps for navigation.

References

[1] P. Long, T. Fan, X. Liao, W. Liu, H. Zhang, and J. Pan, "Towards optimally decentralized multi-robot collision avoidance via deep

reinforcement learning," in *2018 IEEE international conference on robotics and automation (ICRA)*, pp. 6252–6259, IEEE, 2018.
[2] Y. F. Chen, M. Liu, M. Everett, and J. P. How, "Decentralized non-communicating multiagent collision avoidance with deep reinforcement learning," in *2017 IEEE international conference on robotics and automation (ICRA)*, pp. 285–292, IEEE, 2017.
[3] M. Everett, Y. F. Chen, and J. P. How, "Collision avoidance in pedestrian-rich environments with deep reinforcement learning," *IEEE Access*, vol. 9, pp. 10357–10377, 2021.
[4] M. Everett, Y. F. Chen, and J. P. How, "Motion planning among dynamic, decision-making agents with deep reinforcement learning," in *2018 IEEE/RSJ International Conference on Intelligent Robots and Systems (IROS)*, pp. 3052–3059, IEEE, 2018.
[5] S. Dergachev and K. Yakovlev, "Distributed multi-agent navigation based on reciprocal collision avoidance and locally confined multi-agent path finding," in *2021 IEEE 17th International Conference on Automation Science and Engineering (CASE)*, pp. 1489–1494, IEEE, 2021.
[6] A. Kamenev, L. Wang, O. B. Bohan, I. Kulkarni, B. Kartal, A. Molchanov, S. Birchfield, D. Nistér, and N. Smolyanskiy, "Predictionnet: Real-time joint probabilistic traffic prediction for planning, control, and simulation," in *2022 International Conference on Robotics and Automation (ICRA)*, pp. 8936–8942, IEEE, 2022.
[7] S. Le Cleac'h, M. Schwager, and Z. Manchester, "Algames: a fast augmented lagrangian solver for constrained dynamic games," *Autonomous Robots*, vol. 46, no. 1, pp. 201–215, 2022.
[8] R. Chandra, R. Maligi, A. Anantula, and J. Biswas, "Socialmapf: Optimal and efficient multi-agent path finding with strategic agents for social navigation," *arXiv preprint arXiv:2210.08390*, 2022.
[9] J. Alonso-Mora, A. Breitenmoser, M. Rufli, P. Beardsley, and R. Siegwart, "Optimal reciprocal collision avoidance for multiple non-holonomic robots," in *Distributed Autonomous Robotic Systems: The 10th International Symposium*, pp. 203–216, Springer, 2013.
[10] J. Van Den Berg, S. J. Guy, M. Lin, and D. Manocha, "Reciprocal n-body collision avoidance," in *Robotics Research: The 14th International Symposium ISRR*, pp. 3–19, Springer, 2011.
[11] J. Grover, C. Liu, and K. Sycara, "The before, during, and after of multi-robot deadlock," *The International Journal of Robotics Research*, p. 02783649221074718, 2016.
[12] S. H. Arul, J. J. Park, and D. Manocha, "Ds-mpepc: Safe and deadlock-avoiding robot navigation in cluttered dynamic scenes," *arXiv preprint arXiv:2303.10133*, 2023.
[13] L. Wang, A. D. Ames, and M. Egerstedt, "Safety barrier certificates for collisions-free multirobot systems," *IEEE Transactions on Robotics*, vol. 33, no. 3, pp. 661–674, 2017.
[14] Y. Chen, M. Guo, and Z. Li, "Recursive feasibility and deadlock resolution in mpc-based multi-robot trajectory generation," *arXiv preprint arXiv:2202.06071*, 2022.
[15] B. Davis, I. Karamouzas, and S. J. Guy, "Nh-ttc: A gradient-based framework for generalized anticipatory collision avoidance," *arXiv preprint arXiv:1907.05945*, 2019.
[16] X. Xiao, Z. Xu, Z. Wang, Y. Song, G. Warnell, P. Stone, T. Zhang, S. Ravi, G. Wang, H. Karnan, *et al.*, "Autonomous ground navigation in highly constrained spaces: Lessons learned from the benchmark autonomous robot navigation challenge at icra 2022 [competitions]," *IEEE Robotics & Automation Magazine*, vol. 29, no. 4, pp. 148–156, 2022.
[17] J. Grover, C. Liu, and K. Sycara, "Why does symmetry cause deadlocks?," *IFAC-PapersOnLine*, vol. 53, no. 2, pp. 9746–9753, 2020.
[18] D. Zhou, Z. Wang, S. Bandyopadhyay, and M. Schwager, "Fast, online collision avoidance for dynamic vehicles using buffered voronoi cells," *IEEE Robotics and Automation Letters*, vol. 2, no. 2, pp. 1047–1054, 2017.
[19] Z. Zhong, M. Nejad, and E. E. Lee, "Autonomous and semiautonomous intersection management: A survey," *IEEE Intelligent Transportation Systems Magazine*, vol. 13, no. 2, pp. 53–70, 2020.
[20] T.-C. Au, S. Zhang, and P. Stone, "Autonomous intersection management for semi-autonomous vehicles," in *The Routledge handbook of transportation*, pp. 88–104, Routledge, 2015.
[21] D. Carlino, S. D. Boyles, and P. Stone, "Auction-based autonomous intersection management," in *16th International IEEE Conference on Intelligent Transportation Systems (ITSC 2013)*, pp. 529–534, IEEE, 2013.
[22] N. Suriyarachchi, R. Chandra, J. S. Baras, and D. Manocha, "Gameopt: Optimal real-time multi-agent planning and control for dynamic intersections," in *2022 IEEE 25th International Conference on Intelligent Transportation Systems (ITSC)*, pp. 2599–2606, IEEE, 2022.
[23] K. Dresner and P. Stone, "A multiagent approach to autonomous intersection management," *Journal of artificial intelligence research*, vol. 31, pp. 591–656, 2008.
[24] X. Xiao, B. Liu, G. Warnell, and P. Stone, "Motion planning and control for mobile robot navigation using machine learning: a survey," *Autonomous Robots*, vol. 46, no. 5, pp. 569–597, 2022.
[25] M. Wang, Z. Wang, J. Talbot, J. C. Gerdes, and M. Schwager, "Game-theoretic planning for self-driving cars in multivehicle competitive scenarios," *IEEE Transactions on Robotics*, vol. 37, no. 4, pp. 1313–1325, 2021.
[26] A. Britzelmeier, A. Dreves, and M. Gerdts, "Numerical solution of potential games arising in the control of cooperative automatic vehicles," in *2019 Proceedings of the conference on control and its applications*, pp. 38–45, SIAM, 2019.
[27] J. F. Fisac, E. Bronstein, E. Stefansson, D. Sadigh, S. S. Sastry, and A. D. Dragan, "Hierarchical game-theoretic planning for autonomous vehicles," in *2019 International conference on robotics and automation (ICRA)*, pp. 9590–9596, IEEE, 2019.
[28] W. Schwarting, A. Pierson, S. Karaman, and D. Rus, "Stochastic dynamic games in belief space," *IEEE Transactions on Robotics*, pp. 1–16, 2021.
[29] W. Sun, E. A. Theodorou, and P. Tsiotras, "Game theoretic continuous time differential dynamic programming," in *2015 American Control Conference (ACC)*, pp. 5593–5598, IEEE, 2015.
[30] W. Sun, E. A. Theodorou, and P. Tsiotras, "Stochastic game theoretic trajectory optimization in continuous time," in *2016 IEEE 55th Conference on Decision and Control (CDC)*, pp. 6167–6172, IEEE, 2016.
[31] J. Morimoto and C. G. Atkeson, "Minimax differential dynamic programming: An application to robust biped walking," in *Advances in neural information processing systems*, pp. 1563–1570, 2003.
[32] D. Fridovich-Keil, E. Ratner, L. Peters, A. D. Dragan, and C. J. Tomlin, "Efficient iterative linear-quadratic approximations for nonlinear multi-player general-sum differential games," in *2020 IEEE international conference on robotics and automation (ICRA)*, pp. 1475–1481, IEEE, 2020.
[33] B. Di and A. Lamperski, "Differential dynamic programming for nonlinear dynamic games," *arXiv preprint arXiv:1809.08302*, 2018.
[34] B. Di and A. Lamperski, "Newton's method and differential dynamic programming for unconstrained nonlinear dynamic games," in *2019 IEEE 58th Conference on Decision and Control (CDC)*, pp. 4073–4078, IEEE, 2019.
[35] B. Di and A. Lamperski, "First-order algorithms for constrained nonlinear dynamic games," *arXiv preprint arXiv:2001.01826*, 2020.
[36] E. A. Hansen, D. S. Bernstein, and S. Zilberstein, "Dynamic programming for partially observable stochastic games," in *AAAI*, vol. 4, pp. 709–715, 2004.
[37] D. Fox, W. Burgard, and S. Thrun, "The dynamic window approach to collision avoidance," *IEEE Robotics & Automation Magazine*, vol. 4, no. 1, pp. 23–33, 1997.
[38] J. J. Park, C. Johnson, and B. Kuipers, "Robot navigation with model predictive equilibrium point control," in *2012 IEEE/RSJ International Conference on Intelligent Robots and Systems*, pp. 4945–4952, IEEE, 2012.
[39] A. D. Ames, S. Coogan, M. Egerstedt, G. Notomista, K. Sreenath, and P. Tabuada, "Control barrier functions: Theory and applications," in *2019 18th European control conference (ECC)*, pp. 3420–3431, IEEE, 2019.
[40] D. Zhou, Z. Wang, S. Bandyopadhyay, and M. Schwager, "Fast, online collision avoidance for dynamic vehicles using buffered voronoi cells," *IEEE Robotics and Automation Letters*, vol. 2, no. 2, pp. 1047–1054, 2017.
[41] J. W. Grizzle, C. Chevallereau, R. W. Sinnet, and A. D. Ames, "Models, feedback control, and open problems of 3d bipedal robotic walking," *Automatica*, vol. 50, no. 8, pp. 1955–1988, 2014.
[42] R. Chandra and D. Manocha, "Gameplan: Game-theoretic multi-agent planning with human drivers at intersections, roundabouts, and merging," *IEEE Robotics and Automation Letters*, vol. 7, no. 2, pp. 2676–2683, 2022.
[43] A. Wächter and L. T. Biegler, "On the implementation of an interior-point filter line-search algorithm for large-scale nonlinear programming," *Mathematical programming*, vol. 106, pp. 25–57, 2006.
[44] J. Holtz and J. Biswas, "Socialgym: A framework for benchmarking social robot navigation," *arXiv preprint arXiv:2109.11011*, 2021.
[45] J. Zeng, B. Zhang, and K. Sreenath, "Safety-critical model predictive control with discrete-time control barrier function," in *2021 American Control Conference (ACC)*, pp. 3882–3889, IEEE, 2021.
[46] R. Akcelik, "An investigation on pedestrian movement characteristics at mid-block signalised crossings," *Akcelik & Associaties Pty Ltd, Australia*, 2001.
[47] A. Garcimartín, D. R. Parisi, J. M. Pastor, C. Martín-Gómez, and I. Zuriguel, "Flow of pedestrians through narrow doors with different competitiveness," *Journal of Statistical Mechanics: Theory and Experiment*, vol. 2016, no. 4, p. 043402, 2016.